Optimization of Orange-Emitting Electrophosphorescent Copolymers for Organic Light-Emitting Diodes

ARTICLE *in* ADVANCED FUNCTIONAL MATERIALS · OCTOBER 2008

Impact Factor: 11.81 · DOI: 10.1002/adfm.200800446

8 AUTHORS, INCLUDING:

Benoit Domercq
Asahi Glass Company
82 PUBLICATIONS **3,144** CITATIONS
SEE PROFILE

Lauren E Polander
Wiley-VCH Verlag
16 PUBLICATIONS **505** CITATIONS
SEE PROFILE

Seth Marder
Georgia Institute of Technology
667 PUBLICATIONS **26,634** CITATIONS
SEE PROFILE

Bernard Kippelen
Georgia Institute of Technology
437 PUBLICATIONS **12,123** CITATIONS
SEE PROFILE

ADVANCED FUNCTIONAL MATERIALS

FULL PAPER

DOI: 10.1002/adfm.200800446

Optimization of Orange-Emitting Electrophosphorescent Copolymers for Organic Light-Emitting Diodes**

By *Andreas Haldi, Alpay Kimyonok, Benoit Domercq, Lauren E. Hayden, Simon C. Jones, Seth R. Marder,* Marcus Weck,** and *Bernard Kippelen**

Orange-emitting phosphorescent copolymers containing iridium complexes and bis(carbazolyl)fluorene groups in their side chains are employed as the emissive layer in multilayer organic light-emitting diodes (OLEDs). The efficiency of the OLED devices is optimized by varying characteristics of the copolymers: the molecular weight, the iridium loading level, and the nature and length of the linker between the side chains and the polymer backbone. A maximum efficiency of $4.9 \pm 0.4\%$, 8.8 ± 0.7 cd A^{-1} at 100 cd m^{-2} is achieved with an optimized copolymer.

1. Introduction

Phosphorescent organic light-emitting diodes (OLEDs) are currently receiving strong interest since an internal electroluminescence quantum efficiency of almost 100% can be achieved in these devices.[1] While high efficiencies were first achieved in vacuum-deposited OLEDs,[1–3] only recently have comparable efficiencies been measured in solution-processed devices.[4] The performance of these devices has been increased using various approaches, such as synthesizing dendrimers of phosphorescent complexes to afford site isolation of the emissive material,[5] by molecularly doping of a hole-transport polymer with phosphorescent complexes and an electron-transport material,[4,6,7] or by synthesizing copolymers that combine all required elements.[8–12] Processing materials from solution can simplify the fabrication of OLEDs since methods including spin coating, screen printing or inkjet printing can be used. Solution processing of organic materials can potentially enable roll-to-roll processes that could increase production volumes and lower costs.

In molecularly doped OLEDs, the phosphorescent dopant complexes tend to cluster within the doped layers, which can lead to quenching of the luminescence.[13,14] It is possible that this limitation can be circumvented by incorporation of the host material and the organometallic phosphorescent complex in a copolymer. By choosing the right synthetic methodology, it is possible to fabricate copolymers that are derived from monomers with specified functionalities, such as phosphorescent emission, hole- and electron transport, or crosslinking properties. Furthermore, in contrast to many guest–host approaches, copolymers may be less subject to morphological changes, such as phase separation and crystallization, overtime; they, therefore, have the potential for higher stability, especially in applications that require large light output and consequently generate heat under operational conditions. This stability at higher temperatures can also further ease packaging and processing requirements.

OLEDs in which an iridium complex is directly attached to, or even inserted into, the polymer backbone,[10,15,16] generally exhibit low efficiencies, apart from a report by Zhen et al. on a red-emitting chelating copolymer.[10] In a different approach, Evans et al. have demonstrated that polymers with an iridium complex attached to the polymer as a side chain are preferable to achieve high efficiencies in OLED devices.[17] This approach has often been used in the literature and in many cases, iridium complex units (for phosphorescent emission) and carbazole units (for hole transport) have been attached as side groups to vinyl polymer backbones.[9,11,12,18–21] However, the external quantum efficiencies of single-layer devices based on these copolymers rarely exceed 1%. In order to fabricate efficient OLED devices, a hole-blocking and/or electron-transport layer is typically evaporated on top of the emissive copolymer,[18,19] or as Tokito et al. demonstrated, a small molecule with electron-transport properties has to be dispersed in the

[*] Prof. B. Kippelen, Dr. A. Haldi, Dr. B. Domercq
School of Electrical and Computer Engineering, Center of Organic Photonics & Electronics (COPE)
Georgia Institute of Technology
Atlanta, GA 30332-0250 (USA)
E-mail: kippelen@ece.gatech.edu
Prof. M. Weck,[+] Prof. S. R. Marder, Dr. A. Kimyonok, L. E. Hayden, Dr. S. C. Jones
School of Chemistry and Biochemistry, Center of Organic Photonics & Electronics (COPE)
Georgia Institute of Technology
Atlanta, GA 30332-0400 (USA)
E-mail: marcus.weck@nyu.edu; seth.marder@chemistry.gatech.edu
[+] Present address: Department of Chemistry and Molecular Design Institute, New York University, New York, NY 10003-6688, USA

[**] This material is based upon work supported in part by Solvay SA, by the STC Program of the National Science Foundation under Agreement Number DMR-0120967, and by the Office of Naval Research. We thank Chun Huang for assistance in the synthesis of compound **2**, Dr. Yadong Zhang and Dr. Sushanta Pal for the synthesis of compound **9**, and Dr. Stephen Barlow for critical reading of our manuscript.

ADVANCED FUNCTIONAL MATERIALS

copolymer.[9,11] In fact, the highest efficiencies reported for a device with an emissive layer based on copolymers resulted when all three components – hole-transport material, electron-transport material, and emissive material – were copolymerized from side chain monomers.[8,12] Using a polyvinyl backbone with side groups consisting of iridium complexes for emission, *N*,*N*′-diphenyl-*N*,*N*′-bis(3-methylphenyl)-[1,1′-biphenyl]-4,4′-diamine (TPD) for hole transport, and 2-(4-biphenyl)-5-(4-*tert*-butylphenyl)-1,3,4-oxadiazole (PBD) for electron transport, external quantum efficiencies of up to 11.8% have been achieved.[8]

Here, we present a study with the goal of optimizing the efficiency of OLED devices using copolymers in which an orange-emitting iridium complex and a 2,7-di(carbazol-9-yl)fluorene group are attached as side chains. This copolymer was chosen because it showed the highest efficiency in an initial screening of copolymers with different iridium complexes.[22] The efficiency of the OLED devices based on this copolymer was then increased through variations in the molecular weight of the polymer, by changing the iridium concentration in the copolymer, and by varying the nature and the length of the linkage group between the functional side groups and the polymer backbone.

2. Copolymer Design Rationale

Covalent attachment of the host material to the polymer backbone along with the emissive metal complex by randomly copolymerizing two functional monomers in a controlled fashion allows us to combine the properties of both compounds in a single material. Furthermore, the structure of each monomer can be optimized independently without drastically modifying the polymerization reactivity.

To develop fully functionalized copolymers with optimized performance in OLEDs we varied several of their properties, including their iridium concentration, their molecular weight, and the nature and the length of the linker group between the side groups and the polymer backbone. The molecular weight was varied because it may influence processing and the morphology of the films that in turn will impact device performance. Likewise, the concentration of the iridium emitter was varied and optimized to mitigate the adverse effects of concentration quenching and avoid any insufficient energy transfer from host to guest material in the emissive layer, as has been reported previously for evaporated or molecularly doped OLEDs.[23,24]

Finally, the nature and length of the linker group between the side chains and the polymer backbone was varied. While a short spacer between the emissive center and the polymer backbone might be desirable in order to minimize the amount of inactive groups, a long spacer for the emitter may be desirable to achieve better mixing with the host material units. Therefore, in one study we varied the length of the linker between the emitter and the polymer backbone. In another study, we changed the nature of the linker between the hole-transport material and the polymer backbone to address the effect of its polarity on device performance, but we kept its length short. Hence, an ether linker was replaced by a more polar ester linker. Such a substitution can lead to a decrease in the hole mobility[25,26] of the polymer due to the higher polarity of the ester group, leading to better balance between holes and electrons, as suggested previously.[27] The variation of the length of the linker group between the emitter and the backbone was motivated by the work of Evans et al.[17] that suggested that a longer linker could minimize the wavefunction overlap between the organometallic complex and the hole-transport moiety, reducing Dexter triplet energy back-transfer from the emitter to the host material.

3. Results and Discussion

3.1. Synthesis and Characterization

The structure of the monomers **1–4** used to prepare the different polymers are shown in Figure 1. For the host monomers **1** and **2**, we selected an hydroxy-functionalized 2,7-di(carbazol-9-yl)fluorene (compound **6** in Scheme 1) as a building block. Monomer **1**[28] and monomer **2** exhibit similar emission spectra to that of 4,4′-di(carbazol-9-yl)biphenyl (CBP). CBP is one of the most widely used host materials in phosphorescent OLEDs due to its high triplet energy level which enables transfer from both singlet and triplet excitation to a wide range of iridium complexes.[29–31] Indeed, the promising performance of the combination of the bis(carbazolyl)-fluorene host material and an orange-emitting iridium complex in the emissive layer of an OLED device in our previous study indicates an efficient energy transfer from the host to the iridium complex.[22]

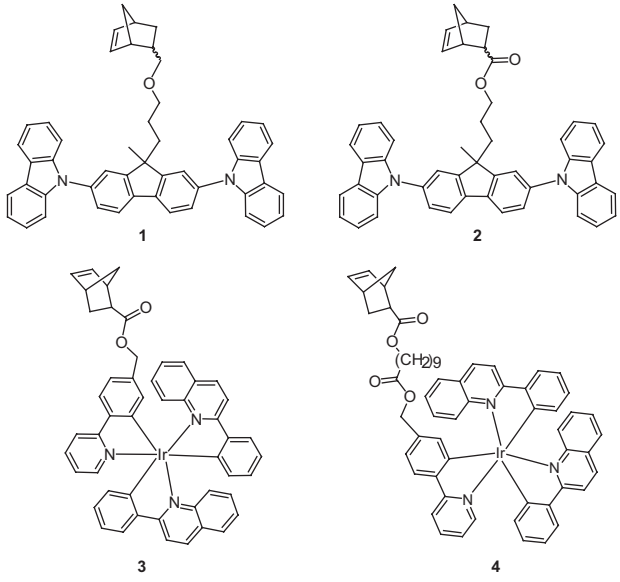

Figure 1. Structures of the monomers.

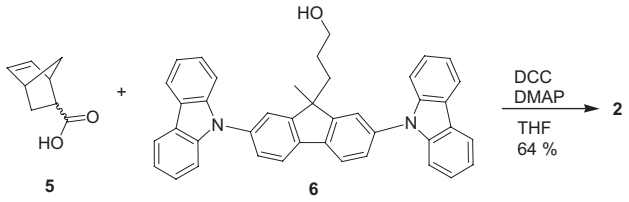

Scheme 1. Synthesis of host monomer **2**.

Monomers **1** and **3** (Fig. 1) were prepared according to literature procedures.[22,28] The host monomer **2** was prepared by coupling of the norbornene acid **5** and compound **6** (Scheme 1) using DCC/DMAP.[28] Monomer **4** was synthesized by the reaction of compound **7**[32] with the alcohol-functionalized iridium complex **8** (Scheme 2).[22]

Copolymerizations of **1** or **2** with **3** or **4** were carried out in chloroform at room temperature using Grubbs' third generation initiator (Scheme 3).[33] All copolymerizations were complete within 10 min. A range of monomer to catalyst ratios as well as ratios of host monomer to iridium monomer were employed in order to obtain polymers with variable molecular weight and iridium content. Table 1 lists the polymer

Table 1. Characterization of copolymers with peak maxima of solid-state photoluminescence (λ_{max}, PL) and electroluminescence spectra (λ_{max}, EL), plus external quantum efficiency (EQE) and luminous efficiency at 100 cd m^{-2} for devices based on phosphorescent copolymers with different molecular weights (*Mn*), different iridium concentrations, and different linkages between the side groups and the polymer backbone. The device structure was ITO/**9** (35 nm)/**P(1–3) (a–c)(2–40)** (20–25 nm)/BCP (40 nm)/LiF (1 nm)/Al.

Polymer	*m*/*n* [mol%]	M_n [kDa]	PDI	$\lambda_{max,PL}$ [nm]	$\lambda_{max,EL}$ [nm]	EQE %	Luminous efficiency [cd A^{-1}]
P1a(10)	89:11	19.0	1.29	594	600	2.9 ± 0.3	3.9 ± 0.4
P1b(10)	92:8	70.0	1.33	590	602	3.2 ± 0.3	4.9 ± 0.4
P1c(10)	90:10	238.0	1.47	591	607	1.5 ± 0.1	2.0 ± 0.1
P1a(2)	98:2	16.0	1.34	595	596	1.9 ± 0.3	2.6 ± 0.4
P1a(5)	95:5	23.0	1.26	605	598	3.4 ± 0.4	4.6 ± 0.5
P1a(7)	93:7	16.0	1.43	597	602	3.0 ± 0.4	4.1 ± 0.5
P1a(15)	81:19	21.0	1.48	605	607	2.4 ± 0.2	3.2 ± 0.3
P1a(20)	79:21	19.5	1.44	604	607	2.0 ± 0.1	2.7 ± 0.2
P1a(30)	75:25	19.5	1.32	612	611	1.9 ± 0.1	2.6 ± 0.1
P1a(40)	71:29	27.0	1.25	613	612	1.7 ± 0.1	2.3 ± 0.1
P2a(10)	90:10	16.0	1.31	592	605	3.9 ± 0.3	5.3 ± 0.4
P3a(10)	90:10	20.0	1.21	594	603	4.5 ± 0.5	8.0 ± 0.9
P3a(5)	95:5	16.5	1.21	595	597	4.9 ± 0.4	8.8 ± 0.7

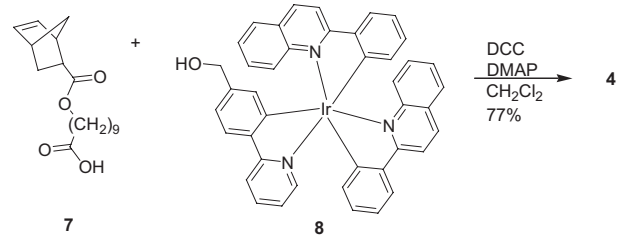

Scheme 2. Synthesis of iridium containing monomer **4**.

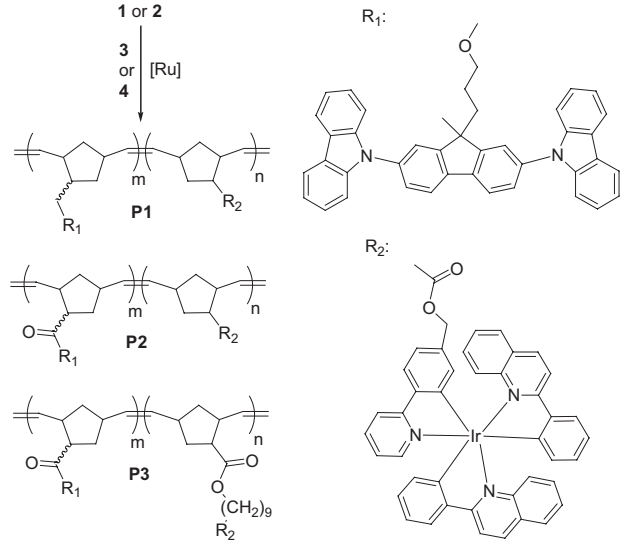

Scheme 3. Synthesis of copolymers **P1**-**P3**.

properties of copolymers **P1–P3**. For **P1a–c**, by varying the monomer to catalyst ratio, we have obtained polymers with molecular weights varying between 19 and 238 kDa, with polydispersities of 1.29–1.47. In the following discussion, we will adopt **P(1–3)(a–c)(n)** as a general nomenclature to refer to the different copolymers that have been synthesized and studied. The first numeric index **(1–3)** is used to identify the polymers as shown in Scheme 3. The second index **(a–c)** refers to the molecular weight range of the copolymer, and finally the third index **(n)** refers to the percentage of iridium-containing monomer relative to the total number monomers used in the polymerization. For copolymers **P1a(2–40)**, we kept the monomer to catalyst ratio constant (50:1 molar ratio) leading to molecular weight in a range comparable to that of polymer **P1a**, but we varied the relative percentages of the iridium-containing monomer in the copolymers from a 98:2 (**2**:**3**) to a 60:40 molar ratio. The incorporation of iridium monomers into the copolymers has been measured using elemental analysis and ranges from 2 to 29 mol % (Table 1). The iridium monomer feed ratios and the measured iridium content in the copolymers are in good agreement for copolymers with less than or equal to 20 mol % Ir monomer. For higher Ir monomer loading levels (30 and 40 mol %), the measured iridium loadings are lower than the theoretical ones (the molar feed ratio for **P1a(40)** was *m*/*n* = 60:40 with an incorporation of *m*/*n* = 71:29 while for **P1a(30)** the molar feed ratio of *m*/*n* = 70:30 resulted in *m*/*n* = 75:25). This may be due to a loss of oligomeric iridium-containing materials that aggregate during purification. It has already been proposed previously that aggregation might occur during the polymerization due to the close proximity of the iridium complexes.[22,34] For lower iridium levels, the host material acts as a spacer between the

ADVANCED FUNCTIONAL MATERIALS

metal complexes preventing, at least partially, potential aggregation.

3.2. Photophysical Properties

The absorption and photoluminescence spectra of **P1a(10)** have been reported previously.[22] Comparable spectra have been measured of copolymers **P1a(10)**, **P1b(10)**, **P1c(10)**, **P2a(10)**, and **P3a(10)** in solid-state and in solution, indicating that the polymer chain length [**P1a(10)**, **P1b(10)**, and **P1c(10)**] and spacer length or type [**P2a(10)** and **P3a(10)**] do not affect the emission properties (Table 1). Increasing the iridium concentration, on the other hand, resulted in a red-shift in the solid-state emission. The photoluminescence spectrum of the polymer with the lowest Ir monomer loading (2 mol %) peaks at 595 nm, whereas the polymer with highest iridium loading (29 mol %) has its maximum at 613 nm. The photoluminescence quantum yield of the iridium-based orange organometallic complex in its small molecule form, its monomer form or even in a copolymer in toluene is ~10% which is low compared to that of the well-known green complex *fac* tris(2-phenylpyridine)iridium [$Ir(ppy)_3$, $\Phi = 0.41$].[20,22,29]

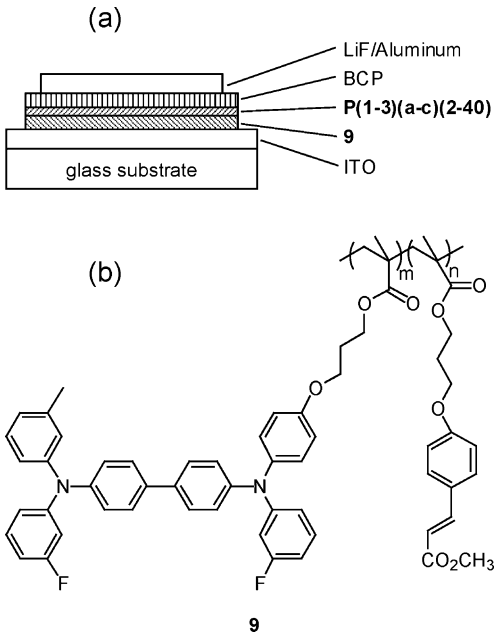

Figure 2. a) Device geometry; b) structure of the crosslinkable hole-transport polymer.

3.3. Organic Light-Emitting Diodes

The most efficient device structures of a solution-processed organic light-emitting diode generally consist of a hole-transport layer, an emissive layer, and a hole-blocking/electron-transport layer.[4] The hole-transport layer facilitates hole-injection into the emissive layer and has to be crosslinked to ensure that it does not dissolve when the emissive layer is spin coated on top of it. The hole-blocking layer confines the holes to the emissive layer, which increases the efficiency significantly. However, the most widely used hole-blocking materials are small molecules, and they are generally processed by physical vapor deposition. The OLED device geometry used in this study is shown in Figure 2a.

In this paper, we employed a TPD-based acrylate copolymer with 20 mol % of a cinnamate crosslinkable moiety as hole-transport material (Fig. 2b); this copolymer was synthesized as previously described.[35] The TPD derivative with two fluoro groups was chosen since this derivative has an increased ionization potential compared to TPD and is known to lead to higher efficiencies in OLEDs.[36,37] During device fabrication, the hole-transport material was spin coated onto oxygen plasma-treated indium tin oxide (ITO)-coated glass and crosslinked under a broadband UV light. The copolymers were then spin coated on top of the hole-transport material, followed by vacuum deposition of bathocuproine (2,9-dimethyl-4,7-diphenyl-1,10-phenanthroline, BCP) as hole-blocking layer, lithium fluoride (LiF) as electron injection layer,[38] and aluminum as the cathode layer.

External quantum efficiencies and luminous efficiencies at 100 cd m^{-2} are listed in Table 1 for the devices fabricated with different copolymers. The efficiency of devices with copolymers of different molecular weights [**P1a-c(10)**] was found to decrease for the copolymers with the highest molecular weight (238 kDa). However, no significant difference in efficiencies could be found when the molecular weight was varied between 19 and 70 kDa.

The study of the dependence of the concentration of the iridium complex in the copolymer [**P1a(2-40)**] showed that the highest efficiency could be achieved for loading levels around 5 mol % (Fig. 3). This is in agreement with several literature reports of similar studies on evaporated or molecularly doped OLEDs.[1,2,7,10,23,24,39,40] The best efficiencies are generally

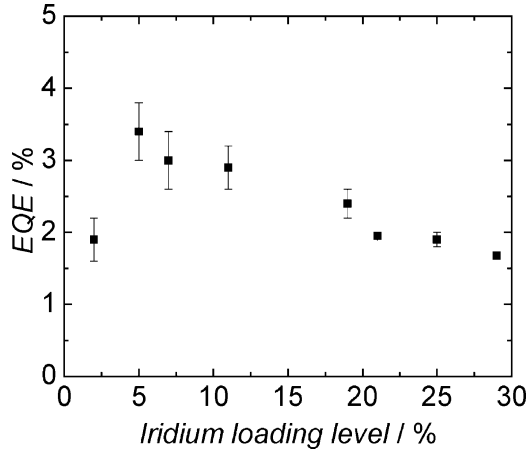

Figure 3. External quantum efficiency (EQE) as a function of the loading level of the iridium complex in the copolymer for OLEDs with device configuration ITO/**9** (35 nm)/**P1a(2-40)** (20-25 nm)/BCP (40 nm)/LiF (1 nm)/Al.

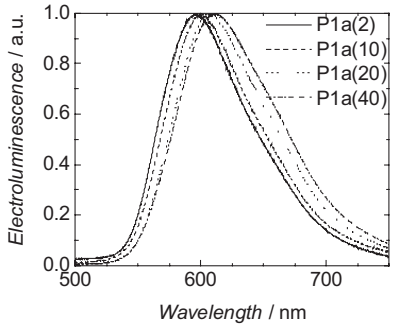

Figure 4. Electroluminescence spectra for OLED devices using **P1a(2, 10, 20, 40)** copolymers with increasing iridium complex content as emitting layer.

reported for iridium complex concentrations below 8 wt %, or 5–6 mol %. For higher loading levels, concentration quenching is expected.[41] For concentrations below 1 wt %, light emission from the host and the guest can be observed simultaneously,[40] indicating that the efficiency of the energy transfer from the host to the guest is reduced. In our case, a red-shift in the electroluminescence spectrum was also observed for increasing iridium concentration, comparable to the red-shift measured in the photoluminescence spectra of these polymers (Fig. 4). While the maximum of the spectrum is at 596 nm for the copolymer with an iridium complex concentration of 5 mol %, it shifts to 612 nm for copolymers with 29 mol % iridium concentration. For the low concentration of 2 mol % a slight shoulder in the spectrum at 500 nm was visible. With a 5 mol % iridium concentration, the Commission International de l'Eclairage (CIE) coordinates of the emission were $x = 0.58$; $y = 0.42$.

In a next step, the influence of linkage between the functional groups and the polymer backbone on the efficiency of the OLEDs was studied. First, the ether group that connects the bis(carbazolyl)fluorene group to the polymer backbone was replaced by an ester group (**P2**). The efficiency of an OLED with **P2a(10)** as the emissive layer was 1% higher at 100 cd m^{-2} than for the copolymer with an ether linkage. Finally, inserting an elongated linkage between the iridium complex and the polymer backbone [**P3a(10)**] increased the EQE by another 0.6%. Because of the low value (10% in toluene) of the photoluminescence quantum yield of the orange iridium emitter,[22] changes in the quantum yield for the copolymers **P(1–3)a(10)** are within the standard deviation of these measurements and no difference could be observed. Potential morphological changes of the thin films based on these copolymers that could influence the efficiency of the devices are currently under investigation.

Combining the results discussed above, a copolymer with an elongated ester linker and an iridium complex concentration of 5 mol % was synthesized [**P3a(5)**]. The external quantum efficiency measured in an OLED based on this copolymer as emissive layer was the highest of the present study: $4.9 \pm 0.4\%$ and 8.8 ± 0.7 cd A^{-1} at 100 cd m^{-2} (Fig. 5). These results validate the trends that were established through our studies in which we varied different properties independently. Given the

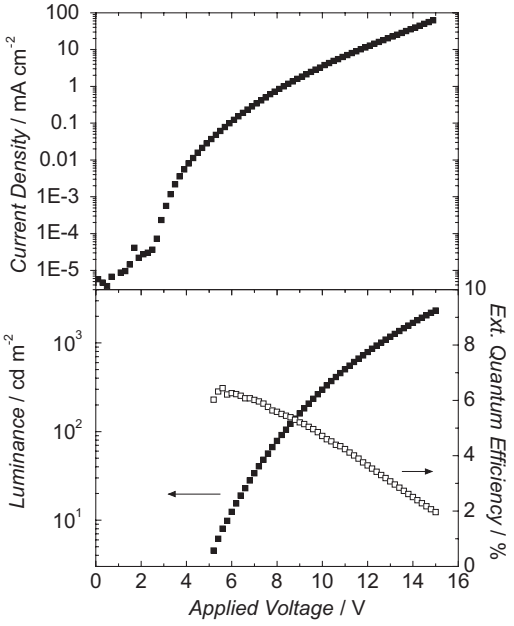

Figure 5. Current density (solid symbols, top), luminance (solid symbols, bottom), and external quantum efficiency (empty symbols, bottom) as a function of applied voltage for a device with structure ITO/**9** (35 nm)/**P3a(5)** (25 nm)/BCP (40 nm)/LiF (1 nm)/Al.

low value of the photoluminescence quantum yield of the orange iridium emitter that was incorporated in these copolymers, the measured EQE of 4.9% with polymer **P3a(5)** indicates that the electroluminescent properties of this copolymer are nearly optimized.

4. Conclusions

Copolymers with an orange iridium complex and bis(carbazolyl)fluorene groups in their side chains were synthesized and incorporated into phosphorescent OLEDs. The chemical nature of these polymers was changed systematically and the effects of these changes on the efficiencies of OLEDs were measured. The molecular weight of the copolymer only displayed significant influence on the efficiency of the device at high molecular weights (>70 kDa). More significant changes in the efficiency could be observed when the loading level of the iridium group was varied. The highest efficiencies were measured in OLEDs based on copolymers with an iridium loading level around 5 mol %. Improvements were found when different linkages were used between the side chains and the polymer backbone. Introducing an ester group into the linkage between the hole-transport group and the polymer backbone also helped to increase the efficiency. Furthermore, the replacement of the short linkage between the iridium complex and the polymer backbone with a longer carbon chain led to an even larger improvement. Efficiencies of $4.9 \pm 0.4\%$ at 100 cd m^{-2} were measured in optimized devices.

ADVANCED FUNCTIONAL MATERIALS

5. Experimental

General Methods: All reagents were purchased either from Acros Organics or Aldrich and used without further purification. ^{1}H NMR and ^{13}C NMR spectra (300 MHz ^{1}H NMR, 75 MHz ^{13}C NMR) were obtained using a Varian Mercury Vx 300 spectrometer. All spectra are referenced to residual proton solvent. Abbreviations used include singlet (s), doublet (d), doublet of doublets (dd), triplet (t), triplet of doublets (td), and unresolved multiplet (m). Mass spectral analyses were provided by the Georgia Tech Mass Spectrometry Facility. Gel-permeation chromatography (GPC) analyses were carried out using a Waters 1525 binary pump coupled to a Waters 2414 refractive index detector with methylene chloride as the eluant on American Polymer Standards 10 μm particle size, linear mixed bed packing columns. The flow rate used for all the measurements was 1 mL min^{-1}. All GPC measurements were calibrated using poly(styrene) standards and carried out at room temperature. UV/Vis absorption measurements were taken on a Shimadzu UV-2401 PC recording spectrophotometer. Emission measurements were acquired using a Shimadzu RF-5301 PC spectrofluorophotometer. Elemental analyses for iridium were provided by Galbraith Laboratories and Atlantic Microlab, Inc.

3-(2,7-Di(9H-carbazol-9-yl)-9-methyl-9H-fluoren-9-yl)propyl bicyclo[2.2.1]hept-5-ene-2-carboxylate: (**2**, ca. 3:1 *endo*/*exo* isomer mixture): *N*,*N*′-dicyclohexylcarbodiimide (1.46 g, 7.03 mmol) was added to a stirred solution of 4-(*N*,*N*-dimethylamino)pyridine (0.078 g, 0.64 mmol), 3-[2,7-di(9*H*-carbazol-9-yl)-9-methyl-9*H*-fluoren-9-yl]propan-1-ol **1** (4.01 g, 7.03 mmol), and bicyclo[2.2.1]hept-5-ene-2-carboxylic acid **5** (0.883 g, 6.39 mmol, mixture of *endo*- and *exo*-isomers) in dry tetrahydrofuran (16 mL) at 0 °C. This mixture was stirred and allowed to warm to room temperature overnight, filtered, and the filtrate poured into H_2O and subsequently extracted with diethyl ether. The combined organic layers were washed with Na_2CO_3 (aq., sat.), NaCl (aq., sat.), and then dried over $MgSO_4$. Volatiles were removed in vacuo to yield an oily off-white solid, which was purified using column chromatography [silica gel, hexanes/ethyl acetate (10:1) elution] to give a white crystalline solid (2.81 g, 64%). ^{1}H NMR (500 MHz, $CDCl_3$): δ 8.18 (d, J = 8.0 Hz, 4H), 8.00 (d, J = 8.0 Hz, 2H), 7.63–7.61 (m, 4H), 7.48–7.43 (m, 8H), 7.30 (t of d, J = ca. 7 Hz, ca. 2 Hz, 4H), 6.01 (m, 1H), 5.89 (d of d, J = 5.5 Hz, 3.0 Hz, ca. 0.3H, *exo*-isomer), 5.77 (d of d, J = 5.5 Hz, 3.0 Hz, ca. 0.7H, *endo*-isomer), 3.90 (t, J = 6.5 Hz, ca. 0.6H, *exo*-isomer), 3.85 (m, ca. 1.4H, *endo*-isomer), 3.03 (br, ca. 0.7H, *endo*-isomer), 2.92 (br, ca. 0.3H, *exo*-isomer), 2.76 (m, ca. 0.6H, *exo*-isomer), 2.72 (br, 1H), 2.15–2.03 (m, overlapping peaks 1H, ca. 1.4H *endo*-isomer), 1.71 (m, 1H), 1.63 (s, 3H), 1.29–1.17 (m, 3H), 1.06 (d, J = 8.5 Hz, ca. 0.7H, *endo*-isomer), 0.95 (d, J = 8.5 Hz, ca. 0.3H, *exo*-isomer), 0.88–0.81 (m, 1H). ^{13}C{^{1}H} NMR (500 Mz, $CDCl_3$): δ 176.0, 175.1, 154.0, 141.4, 139.0, 138.3, 138.2, 137.5, 136.0, 132.6, 126.8, 126.5, 123.9, 122.1, 122.0, 121.8, 120.9, 120.5, 110.2, 64.4, 51.4, 49.9, 46.9, 46.7, 46.1, 43.6, 43.4, 42.8, 41.9, 37.4, 35.1, 30.8, 29.5, 27.1, 25.7, 24.7, 23.1. MS (EI): m/z 688 ([M]$^+$). Anal. Calcd for $C_{49}H_{40}N_2O_2$: C, 85.44; H, 5.85; N, 4.07. Found: C, 84.46; H, 6.18; N, 3.89.

*Fac-exo-bis(2-phenyl-quinolinato, N, C2′){2-[4′-(10-methoxy-10-oxodecyl bicyclo[2.2.1]hept-5-ene-2-carboxyl) phenyl]pyridinato, N, C2′} iridium(III) (**4**)*: Compounds **7** [32] (98 mg, 0.31 mmol) and **8** [22] (200 mg, 0.25 mmol) and dimethylaminopyridine (17 mg, 0.14 mmol) were combined in 10 mL of CH_2Cl_2. A solution of dicyclohexylcarbodiimide (60 mg, 0.30 mmol) in 2 mL of CH_2Cl_2 was added and the reaction was stirred under argon at ambient temperatures for 24 h. The solvent was evaporated and the residue was purified via column chromatography (silica, CH_2Cl_2) to give compound **4** as an orange powder (210 mg, 77% yield). ^{1}H NMR ($CDCl_3$): δ = 8.19 (d, 1H, J = 9 Hz), 8.09 (m, 3H), 7.99 (d, 1H, J = 9 Hz), 7.88 (m, 2H), 7.67 (m, 2H), 7.62 (m, 2H), 7.56 (d, 1H, J = 8.7 Hz), 7.47 (m, 1H), 7.38 (d, 1H, J = 8.1 Hz), 7.19 (m, 3H), 6.92 (m, 3H), 6.73 (m, 4H), 6.63 (m, 2H), 6.45 (d, 1H, J = 1.8 Hz), 6.13 (m, 2H), 4.72 (s, 2H), 4.09 (t, 2H, J = 6.9 Hz), 3.05 (s, 1H), 2.92 (s, 1H), 2.24 (t, 2H, J = 7.5), 1.95 (m, 1H), 1.58 (m, 6H), 1.34 (m, 12H). ^{13}C NMR ($CDCl_3$): δ = 176.6, 173.9, 167.4, 165.8, 163.2, 160.6, 158.4, 149.2, 148.7, 148.2, 146.5, 144.9, 143.6, 138.3, 137.6, 137.1, 137.0, 136.3, 136.1, 135.9, 133.1, 130.4, 129.8, 129.6, 129.2, 128.4, 127.9, 127.8, 127.7, 127.1, 126.4, 126.3, 125.8, 125.3, 123.5, 122.3, 120.6, 120.2, 119.6, 119.1, 118.4, 118.2, 66.6, 64.9, 46.9, 46.6, 43.5, 41.9, 34.6, 30.6, 29.6, 29.5, 29.4, 29.3, 28.9, 26.2, 25.1. MS (ESI): m/z 1008.3 ([M–C_5H_7]). Anal. Calcd. ($C_{60}H_{56}IrN_3O_4$): C, 67.02; H, 5.25; N, 3.91. Found: C, 67.07; H, 5.43; N, 4.12.

General Polymerization Procedure: A solution of Grubbs' third generation initiator [33] in chloroform (0.05 M) was added to a chloroform solution (0.01 M) containing a mixture of monomers **3** or **4** and **1** or **2** in the desired ratios (Table 1). The reaction mixture was stirred for 15 min at ambient temperatures. After 15 min, the polymerization was quenched by the addition of ethyl vinyl ether. The reaction mixture was concentrated and precipitated into methanol. The resulting solid was collected by filtration, redissolved in CH_2Cl_2, and reprecipitated into methanol. This procedure was repeated until the methanol solution was clear to yield copolymers **P1–P3** for which ^{1}H NMR spectra showed no remaining monomer or other impurity signals.

Copolymer **P2**: ^{1}H NMR ($CDCl_3$): δ = 8.07 (br), 7.81 (br), 7.40 (br), 7.23 (br), 6.79 (br), 6.63(br), 5.02 (br), 4.71 (br), 3.78 (br), 2.56 (br), 1.90 (br), 1.49 (br), 1.12 (br). ^{13}C NMR ($CDCl_3$): δ = 167.0, 165.2, 160.3, 158.1, 153.3, 148.7, 145.9, 144.5, 143.0, 140.6, 138.1, 137.2, 136.7, 130.0, 129.3, 128.1, 127.5, 125.9, 125.3, 123.2, 121.5, 121.2, 120.4, 119.8, 117.7, 109.8, 66.4, 63.8, 50.9, 41.7, 36.7, 26.6, 24.4.

Copolymer **P3**: ^{1}H NMR ($CDCl_3$): δ = 8.06 (br), 7.84 (br), 7.48 (br), 7.21 (br), 6.89 (br), 6.68 (br), 4.99 (br), 4.74 (br), 3.72 (br), 2.64 (br), 1.95 (br), 1.50 (br), 1.09 (br). ^{13}C NMR ($CDCl_3$): δ = 167.5, 165.6, 163.1, 160.5, 158.5, 153.7, 149.2, 148.8, 148.2, 146.5, 144.9, 143.6, 141.1, 138.8, 137.6, 137.2, 136.3, 133.1, 132.4, 130.5, 129.8, 128.4, 127.9, 126.5, 123.7, 121.9, 121.6, 120.7, 120.4, 119.7, 119.1, 118.2, 110.0, 66.8, 64.3, 60.7, 51.2, 49.7, 46.2, 45.8, 43.6, 42.5, 37.0, 34.9, 32.1, 29.7, 26.9, 25.5, 24.4, 22.9.

Organic Light-Emitting Diodes: 35 nm thick films of the hole-transport material were spin coated from toluene onto oxygen plasma-treated ITO-coated glass substrates with a sheet resistance of 20 Ω/square (Colorado Concept Coatings, L.L.C.). Films were crosslinked using a standard broad-band UV light with a 0.7 mW cm^{-2} power density for 1 min. Subsequently, a 20–25 nm thick film of the phosphorescent copolymer was spin coated from chloroform on top of the crosslinked hole-transport layer. For the hole-blocking layer, bathocuproine (BCP) was first purified using gradient zone sublimation, and a film of 40 nm was then thermally evaporated at a rate of 0.4 Å s^{-1} and at a pressure below 1×10^{-7} Torr on top of the emissive layer. Lithium fluoride (1 nm) (LiF) and a 200 nm-thick aluminum cathode were vacuum deposited at a pressure below 1×10^{-6} Torr and at rates of 0.1 and 2 Å s^{-1}, respectively. A shadow mask was used for the evaporation of the metal to form five devices with an area of 0.1 cm^2 per substrate. At no point during fabrication were the devices exposed to atmospheric conditions. The testing was done immediately after the deposition of the metal cathode in inert atmosphere without exposing the devices to air.

Received: March 31, 2008
Revised: June 27, 2008
Published online: September 22, 2008

[1] C. Adachi, M. A. Baldo, M. E. Thompson, S. R. Forrest, *J. Appl. Phys.* **2001**, *90*, 5048.
[2] M. A. Baldo, S. Lamansky, P. E. Burrows, M. E. Thompson, S. R. Forrest, *Appl. Phys. Lett.* **1999**, *75*, 4.
[3] T. Tsutsui, M. J. Yang, M. Yahiro, K. Nakamura, T. Watanabe, T. Tsuji, Y. Fukuda, T. Wakimoto, S. Miyaguchi, *Jpn. J. Appl. Phys, Part 2* **1999**, *38*, L1502.

[4] X. H. Yang, D. C. Muller, D. Neher, K. Meerholz, *Adv. Mater.* **2006**, *18*, 948.
[5] S. C. Lo, N. A. H. Male, J. P. J. Markham, S. W. Magennis, P. L. Burn, O. V. Salata, I. D. W. Samuel, *Adv. Mater.* **2002**, *14*, 975.
[6] S. W. Kim, J. H. Park, S. S. Oh, D. Y. Kim, E. H. Choi, G. S. Cho, Y. H. Seo, S. O. Kang, B. Park, Y. Saito, N. Watanabe, H. Takezoe, J. Watanabe, *Appl. Phys. Lett.* **2006**, *89*, 213511.
[7] F. I. Wu, H. J. Su, C. F. Shu, L. Y. Luo, W. G. Diau, C. H. Cheng, J. P. Duan, G. H. Lee, *J. Mater. Chem.* **2005**, *15*, 1035.
[8] M. Suzuki, S. Tokito, F. Sato, T. Igarashi, K. Kondo, T. Koyama, T. Yamaguchi, *Appl. Phys. Lett.* **2005**, *86*, 103507.
[9] S. Tokito, M. Suzuki, F. Sato, M. Kamachi, K. Shirane, *Org. Electron.* **2003**, *4*, 105.
[10] H. Y. Zhen, C. Luo, W. Yang, W. Y. Song, B. Du, J. X. Jiang, C. Y. Jiang, Y. Zhang, Y. Cao, *Macromolecules* **2006**, *39*, 1693.
[11] S. Tokito, M. Suzuki, F. Sato, *Thin Solid Films* **2003**, *445*, 353.
[12] L. Deng, P. T. Furuta, S. Garon, J. Li, D. Kavulak, M. E. Thompson, J. M. J. Frechet, *Chem. Mater.* **2006**, *18*, 386.
[13] F.-C. Chen, G. He, Y. Yang, *Appl. Phys. Lett.* **2003**, *82*, 1006.
[14] W. G. Zhu, Y. Q. Mo, M. Yuan, W. Yang, Y. Cao, *Appl. Phys. Lett.* **2002**, *80*, 2045.
[15] A. J. Sandee, C. K. Williams, N. R. Evans, J. E. Davies, C. E. Boothby, A. Kohler, R. H. Friend, A. B. Holmes, *J. Am. Chem. Soc.* **2004**, *126*, 7041.
[16] S. J. Liu, Q. Zhao, Y. Deng, Y. J. Xia, J. Lin, Q. L. Fan, L. H. Wang, W. Huang, *J. Phys. Chem. C* **2007**, *111*, 1166.
[17] N. R. Evans, L. S. Devi, C. S. K. Mak, S. E. Watkins, S. I. Pascu, A. Kohler, R. H. Friend, C. K. Williams, A. B. Holmes, *J. Am. Chem. Soc.* **2006**, *128*, 6647.
[18] C. L. Lee, N. G. Kang, Y. S. Cho, J. S. Lee, J. J. Kim, *Opt. Mater.* **2003**, *21*, 119.
[19] X. D. Wang, K. Ogino, K. Tanaka, H. Usui, *IEEE J. Sel. Top. Quantum Electron.* **2004**, *10*, 121.
[20] X. Y. Wang, A. Kimyonok, M. Weck, *Chem. Commun.* **2006**, 3933.
[21] X. Y. Wang, R. N. Prabhu, R. H. Schmehl, M. Weck, *Macromolecules* **2006**, *39*, 3140.
[22] A. Kimyonok, B. Domercq, A. Haldi, J.-Y. Cho, J. R. Carlise, X.-Y. Wang, L. E. Hayden, S. C. Jones, S. Barlow, S. R. Marder, B. Kippelen, M. Weck, *Chem. Mater.* **2007**, *19*, 5602.
[23] M. A. Baldo, C. Adachi, S. R. Forrest, *Phys. Rev. B* **2000**, *62*, 10967.
[24] X. Gong, M. R. Robinson, J. C. Ostrowski, D. Moses, G. C. Bazan, A. J. Heeger, *Adv. Mater.* **2002**, *14*, 581.
[25] E. Bellmann, S. E. Shaheen, S. Thayumanavan, S. Barlow, R. H. Grubbs, S. R. Marder, B. Kippelen, N. Peyghambarian, *Chem. Mater.* **1998**, *10*, 1668.
[26] P. M. Borsenberger, L. Pautmeier, R. Richert, H. Bassler, *J. Chem. Phys.* **1991**, *94*, 8276.
[27] J. P. J. Markham, I. D. W. Samuel, S. C. Lo, P. L. Burn, M. Weiter, H. Bassler, *J. Appl. Phys.* **2004**, *95*, 438.
[28] J. Y. Cho, B. Domercq, S. Barlow, K. Y. Suponitsky, J. Li, T. V. Timofeeva, S. C. Jones, L. E. Hayden, A. Kimyonok, C. R. South, M. Weck, B. Kippelen, S. R. Marder, *Organometallics* **2007**, *26*, 4816.
[29] S. Lamansky, P. Djurovich, D. Murphy, F. Abdel-Razzaq, H. E. Lee, C. Adachi, P. E. Burrows, S. R. Forrest, M. E. Thompson, *J. Am. Chem. Soc.* **2001**, *123*, 4304.
[30] A. Tsuboyama, H. Iwawaki, M. Furugori, T. Mukaide, J. Kamatani, S. Igawa, T. Moriyama, S. Miura, T. Takiguchi, S. Okada, M. Hoshino, K. Ueno, *J. Am. Chem. Soc.* **2003**, *125*, 12971.
[31] M. K. Nazeeruddin, R. Humphry-Baker, D. Berner, S. Rivier, L. Zuppiroli, M. Graetzel, *J. Am. Chem. Soc.* **2003**, *125*, 8790.
[32] C. R. South, M. N. Higley, K. C.-F. Leung, D. Lanari, A. Nelson, R. H. Grubbs, J. F. Stoddart, M. Weck, *Chem. Eur. J.* **2006**, *12*, 3789.
[33] J. A. Love, J. P. Morgan, T. M. Trnka, R. H. Grubbs, *Angew. Chem, Int. Ed.* **2002**, *41*, 4035.
[34] J. R. Carlise, X. Y. Wang, M. Weck, *Macromolecules* **2005**, *38*, 9000.
[35] R. D. Hreha, Y. D. Zhang, B. Domercq, N. Larribeau, J. N. Haddock, B. Kippelen, S. R. Marder, *Synthesis* **2002**, *9*, 1201.
[36] B. Domercq, R. D. Hreha, Y. D. Zhang, N. Larribeau, J. N. Haddock, C. Schultz, S. R. Marder, B. Kippelen, *Chem. Mater.* **2003**, *15*, 1491.
[37] A. Haldi, B. Domercq, B. Kippelen, R. D. Hreha, J. Y. Cho, S. R. Marder, *Appl. Phys. Lett.* **2008**, *92*, 253502.
[38] L. S. Hung, C. W. Tang, M. G. Mason, *Appl. Phys. Lett.* **1997**, *70*, 152.
[39] X. Gong, J. C. Ostrowski, D. Moses, G. C. Bazan, A. J. Heeger, *Adv. Funct. Mater.* **2003**, *13*, 439.
[40] X. H. Yang, D. Neher, *Appl. Phys. Lett.* **2004**, *84*, 2476.
[41] G. Ramos-Ortiz, Y. Oki, B. Domercq, B. Kippelen, *Phys. Chem. Chem. Phys.* **2002**, *4*, 4109.